

1 **Comparative assessment of n-butanol addition in CTL on performance and**  
2 **exhaust emissions of a CI engine**

3

4 Wanchen Sun <sup>a</sup>, Yi Sun <sup>a</sup>, Liang Guo <sup>a</sup>, Hao Zhang <sup>a\*</sup>, Yuying Yan <sup>b</sup>, Wenpeng Zeng <sup>a</sup>, Shaodian Lin <sup>a</sup>

5 <sup>a</sup> *State Key Laboratory of Automotive Simulation and Control, Jilin University, Changchun 130025,*  
6 *China*

7 <sup>b</sup> *Faculty of Engineering, the University of Nottingham, Nottingham, UK, NG7 2RD*

8

9 **Abstract**

10 Coal to liquid (CTL) is a diesel alternative fuel based on Fischer-Tropsch (FT) process, which  
11 has shown promising application value. Besides, as an oxygenated biofuel with high oxygen content  
12 and volatility, n-butanol can be blended with hydrocarbon fuels to improve engine performance.  
13 This study aims to investigate the effects of CTL/n-butanol blends on the performance of the  
14 compression-ignition (CI) engine, and to reveal the influence of combustion boundary conditions  
15 such as n-butanol blending ratio, the start of injection (SOI), and exhaust gas recirculation (EGR)  
16 on the combustion and emissions characteristics. The results show that blending n-butanol with CTL  
17 is beneficial to improve the fuel-gas mixture distribution in the cylinder, and the premixed  
18 combustion ratio (PCR) increases by 13.66% as the energy ratio of n-butanol increases to 30% (B30)

---

\* Corresponding author, Address for correspondence: State Key Laboratory of Automotive Simulation and Control, Jilin University, Changchun 130025, People's Republic of China.

*E-mail address:* haoz18@mails.jlu.edu.cn (Hao Zhang).

19 compared with the pure CTL. CTL/n-butanol blends make particulate emission tend to be shifted  
 20 towards nucleation mode and the particulate mass emission significantly reduced, especially the  
 21 particulate mass of B30 reduce by 68.6%; meanwhile, the NO<sub>x</sub> emission shows an upward trend.  
 22 Compared with n-butanol blended, adjusting the SOI impacts NO<sub>x</sub> emissions significantly, while  
 23 its influence on the indicated thermal efficiency (ITE) and particulate emissions is relatively slight.  
 24 Moreover, through the synergistic control of n-butanol addition and EGR, the trade-off relationship  
 25 between NO<sub>x</sub> and particles is mitigated.

26

27 **Highlights:**

- 28 ● CTL facilitates lower the PCR and results in increased particle emissions.
- 29 ● N-butanol blended suppresses the particle emissions from the combustion of CTL.
- 30 ● N-butanol blended promotes the shifting of particles towards the nucleation mode.
- 31 ● The trade-off relationship between NO<sub>x</sub> and particle is mitigated by using EGR and n-butanol.

32

33 *Keywords:* Coal to liquid; N-butanol; Combustion process; Particulate mode; Pollutant emissions

34

<b>Abbreviations</b>			
CTL	Coal to liquid	BTDC	Before top dead center
FT	Fischer-Tropsch	PCR	Premixed combustion ratio
CN	Cetane number	ITE	Indicated thermal efficiency
CI	Compression-ignition	CD	Combustion duration
ESC	European stationary cycle	CA	Crank angle
ID	Ignition delay	CA50	Gravity of heat release

HRR	Heat release rate	NMP	Nucleation mode particle
EGR	Exhaust gas recirculation	AMP	Accumulation mode particle
SOI	Start of injection	TDC	Top dead center
ECU	Electronic control unit	SHC	Specific heat capacity
IMEP	Indicated mean effective pressure	CMD	Count median diameter

## 35 1. Introduction

36 For a long time, fossil energy has played a pivotal role in various fields, such as industry,  
37 agriculture, and transportation [1, 2]. According to the U.S. Energy Department, the global energy  
38 demand has grown since the Industrial Revolution, and more than a billion barrels of oil per day  
39 will be consumed by 2035 [3, 4]. The world is facing severe energy problems, so the search for  
40 alternative energy sources and the efficient use of energy have become a worldwide challenge [5].  
41 At the same time, the increasingly serious environmental pollution and global carbon emissions  
42 have also attracted attention from all walks of life [6, 7]. Obviously, the transportation field  
43 consumes a large amount of fuel (greater than 25% of total) and is also the primary source of  
44 environmental pollution problems. For the automotive industry, which is required to meet the  
45 regulations of fuel consumption and pollutant emission [8, 9], and it is essential to develop energy  
46 diversification strategies based on the local resource endowment.

47 In recent years, numerous researches have been conducted on alternative fuels for automobiles.  
48 Natural gas, hydrogen, biomass fuels, synthetic fuels, etc., have shown good potential as alternative  
49 fuels for gasoline and diesel engines [10-13]. With coal as the primary raw material in many  
50 countries such as China, coal to liquid (CTL) is a high-quality and clean alternative fuel produced  
51 by chemical processing and synthesis technology [14]. A lot of research has been done on CTL in

52 the field of economy and technology, and a more comprehensive evaluation of CTL technology has  
53 been made from the aspects of resource consumption, economic cost, and environmental pollution  
54 [15, 16]. With the progress in coal catalytic conversion technology and emission reduction  
55 technology, the resource utilization rate of coal liquefaction technology has been upgraded, the  
56 carbon emissions of that have been greatly reduced, and the economic cost of CTL has reached a  
57 level comparable to that of the petroleum-based fuels [17, 18]. In addition, because the direct use of  
58 coal would lower energy utilization efficiency and cause considerable emissions that account for the  
59 main source of air pollution, the efficient and clean use of coal resources through synthetic  
60 technology is also of strategic significance [19]. The core reaction of CTL production is the Fischer-  
61 Tropsh (FT) synthesis reaction, and the CTL produced by FT synthesis is mainly composed of  
62 saturated alkane [20]. CTL has the characteristics of high cetane number (CN), low sulfur, low  
63 nitrogen, and low aromatic content, so CTL is a high-quality diesel alternative fuel [21]. Besides,  
64 CTL can be intermixed with conventional petroleum-based fuels in any ratio, making it compatible  
65 with the existing automotive technology systems and having broad application prospects in internal  
66 combustion engines [22, 23]. Song C et al. studied the effects of FT diesel on compression-ignition  
67 (CI) engines under the European stationary cycle (ESC) and constant speed/varying load test  
68 conditions, and the results show that burning FT diesel is beneficial to reduce engine pollutant  
69 emissions [24]. Research by Dai YL et al. showed that when burning CTL liquefied by FT method,  
70 the ignition delay (ID) is shorter, the peak heat release of the premixed combustion is lower, and the  
71 use of CTL can effectively reduce the soot emissions [25].

72 In addition, oxygen fuels such as biodiesel, alcohols, esters, ethers, etc., have also become  
73 research hotspots due to their potential for high-efficient and clean combustion [26-28]. In particular,

74 butanol can be produced through the fermentation of agricultural waste and other biomass [29].  
75 Compared with low-carbon alcohols such as methanol and ethanol, butanol has the characteristics  
76 of high calorific value, high CN, high density, high viscosity, and good lubricity. At the same time,  
77 it has better miscibility with alkane fuels. As an additive, butanol has excellent potential for  
78 application in the CI engine [30-32]. Since the butanol molecule contains oxygen atoms, blending  
79 butanol with diesel helps to increase the oxygen content of the fuel so that it can reduce the emissions  
80 such as particles from CI engines [33-35]. Many research teams used butanol as an additive to blend  
81 with diesel, biodiesel, etc., to explore the potential of achieving high-efficiency and clean  
82 combustion for internal combustion engines by improving fuel characteristics [36-38]. Rajesh  
83 Kumar B et al. studied the effects of butanol/diesel blends on the combustion and emission  
84 characteristics of CI engines in a low-temperature premixed combustion mode, showing that butanol  
85 blended resulted in a longer ID and a higher premixed heat release rate (HRR), and combining with  
86 exhaust gas recirculation (EGR) technology can simultaneously reduce the NO<sub>x</sub> and smoke  
87 emissions of the engine [39]. Chen Z et al. found that the combination of high butanol/diesel  
88 blending ratio and medium EGR ratio has the potential to achieve extremely low NO<sub>x</sub> and soot  
89 emissions while maintaining a high level of thermal efficiency [40]. Huang et al. investigated the  
90 particle emission characteristics of diesel/n-butanol under different EGR conditions, the results  
91 showed that the addition of n-butanol to the fuel makes both the soot emissions and the average  
92 geometric size of particles decrease for EGR ratios smaller than 20%, while the total particle number  
93 concentration of D70B30 compared to D100 reduces by 74.7% at large EGR ratios [41].

94 In order to solve the problems of the short ID and the insufficient premixed combustion of  
95 burning pure CTL in the CI engine, the method of blending n-butanol with CTL was adopted to

96 change the physicochemical properties of the fuel to explore the effects of the CTL/n-butanol blends  
97 on the combustion and emissions characteristics of a CI engine. The combustion boundary  
98 conditions such as the n-butanol blending ratio, the start of injection (SOI), and the EGR ratio were  
99 adjusted to reveal the potential of CTL/n-butanol blends to reduce pollutant emissions, especially  
100 particulate emissions.

## 101 **2. Experimental system and test procedure**

### 102 *2.1 Experimental engine and apparatus*

103 The experimental engine is a single-cylinder CI engine modified from a four-cylinder four-  
104 valve high-pressure common-rail diesel engine, and the main specifications of the engine are shown  
105 in Table 1. In order to flexibly control the SOI and the intake charge, the second cylinder of the  
106 experimental engine is equipped with an independent direct-injection system and intake/exhaust  
107 system, while the other three cylinders are not supplied with fuel. The open electronic control unit  
108 (ECU) is used to control the direct-injection system, and the ECU-NI2106 can achieve flexible  
109 control of the SOI and the injection mass. In addition, the intake/exhaust system consists of a two-  
110 stage simulated supercharge system and an EGR system. The two-stage simulated supercharge  
111 system uses an air compressor as the intake air source, and a two-stage pressure surge chamber  
112 stabilizes the high-pressure air from the compressor. The intake pressure of the engine is flexibly  
113 adjusted between 0 MPa and 0.3 MPa (gauge pressure) by a pressure sensor and a flow-limiting  
114 valve. The EGR system stabilizes the pressure of the exhaust surge chamber by adjusting the  
115 opening of the exhaust backpressure valve and then controls the EGR ratio (up to 30%) by adjusting  
116 the EGR valve.

117 **Table 1.** Engine specifications

Category	Properties
Geometric compression ratio	17.1
Cylinder diameter / mm	95.4
Piston stroke / mm	104.9
Connecting rod length / mm	162
The number of nozzles holes	7
Injector orifice diameter / mm	0.12
Oil jet cone angle / (°)	12
Swirl number	0.97
The shape of combustion chamber	$\omega$

118 The measurement and control equipment used in the engine test platform mainly includes the  
119 eddy current dynamometer, the in-cylinder pressure transducer, the fuel flow meter, the airflow  
120 meter, the fast NO<sub>x</sub> analyzer, the fast HC analyzer, the fast CO&CO<sub>2</sub> analyzer, the electron particle  
121 spectrometer. The cylinder pressure is collected by a combustion analyzer at 0.1° CA intervals and  
122 averaged over 50 cycles at each operating point to eliminate measurement errors. The schematic  
123 diagram of the experimental setup is shown in **Fig. 1**, and the main parameters of the equipment are  
124 shown in **Table 2**.

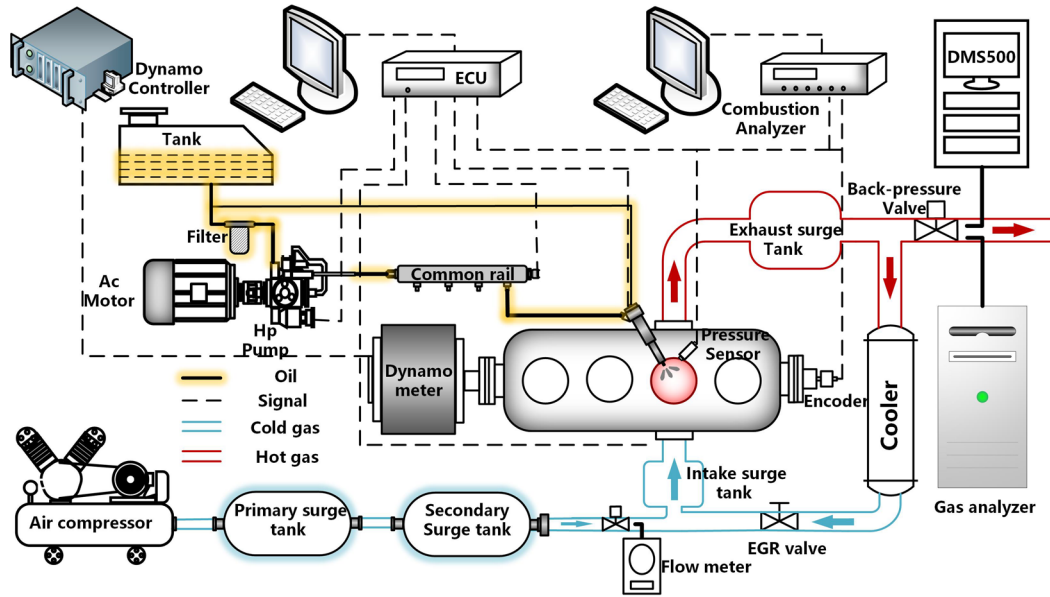


Fig. 1 Schematic diagram of experimental setup

125

Table 2. Main equipment

Category	Measuring instruments	Manufacturer	Accuracy
Dynamometer	CW260	CAMA	Torque: $\pm 0.5$ NM Speed: $\pm 2$ r/min
Rotary encoder	S4001	Bangman	—
Fuel flow meter	FX-100	ONO-SOKKI	$\pm 0.12\%$
Air flow meter	20R100	TOCEL	$\pm 1\%$
Cylinder pressure	6052C	Kistler	$\pm 1\%$
CO&CO <sub>2</sub>	NDIR500	Cambustion	$< 2\%$ FS/hour
HC	HFR500	Cambustion	$< 1\%$ FS/hour
NO <sub>x</sub>	CLD500	Cambustion	$< 5$ ppm/hour
Particle	DMS500	Cambustion	—



126 *2.2 Methodology and test conditions*

127 The basic fuels used in the experiment are low sulfur diesel, CTL, and n-butanol. The main  
128 physicochemical properties of the basic fuels are shown in **Table 3**, the basic parameters are  
129 measured at 25°C. In addition, this study adopts CTL/n-butanol blended fuels defined as BXX, of  
130 which the XX represents the calorific value percentage of n-butanol. For example, the blended fuel  
131 composed of 70% CTL and 30% n-butanol (by calorific value) is defined as B30. Moreover, the  
132 engine operating conditions are shown in **Table 4**. The engine worked at the maximum torque speed  
133 of 1400 r/min, and the load rate was about 50% (the indicated mean effective pressure (IMEP) was  
134 about 0.85 MPa). When comparing between different fuels, the calorific values of CTL and its  
135 blends were kept the same as the calorific value of diesel (1438 J/cycle), so n-butanol ratio of the  
136 blended fuels were set to 10%, 20%, and 30% based on energy ratio. In the experiments, SOI was  
137 selected from 5°CA before top dead center (BTDC) to 13 °CA BTDC with the step of 2 °CA, and  
138 the EGR ratio was selected from 0% to 30% with the step of 10%. Moreover, the EGR ratio was  
139 defined as the ratio of the CO<sub>2</sub> content in the intake and that in the exhaust of the engine, and the  
140 CO<sub>2</sub> content was measured by the exhaust gas analyzer. In addition, when adjusting the EGR ratio  
141 during the experiment, the pure air flow rate (35 kg/h) into the intake remained unchanged, and the  
142 EGR ratio was adjusted by controlling the mass of introduced exhaust gas.

143 The DMS500 measures the particle size/number distribution in an engine exhaust. However,  
144 particle mass has been long established as a metric for legislative measurements of particle  
145 emissions from engines, but particle mass and particle number measurements do not demonstrate a  
146 direct correlation. Therefore, given a size/number distribution, it is desirable to calculate in real-  
147 time a mass concentration, so the conversion equation is as follows:

148

$$Mass(\mu\text{g}) = \text{Density Factor} \cdot Dp^{\text{power factor}}$$

149

For Diesel engine agglomerates, research shows that the DMS500 mass calculation gives good

150

agreement with gravimetric techniques using a density factor of  $2.2 \cdot 10^{-15}$  and a power factor of 2.65.

151

**Table 3.** Main properties of tested fuels

Fuel property	CTL	N-butanol	Diesel	B10	B20	B30
Density under 25°C/ (kg·m <sup>-3</sup> )	757.0	805.5	840.0	763.1	768.9	774.3
Cetane number (CN)	75.4	25	52.9	69.4	63.6	58.1
Low calorific value / (MJ·kg <sup>-1</sup> )	43.07	33.19	42.69	41.89	40.76	39.68
Total Aromatics / %	≤ 0.8	0	≤ 3.6	≤ 0.7	≤ 0.6	≤ 0.5
Latent heat of vaporization / (kJ·kg <sup>-1</sup> )	~	626	270	~	~	~
Sulfur content / 10 <sup>-6</sup>	0.38	0	3.7	0.33	0.29	0.25
Oxygen mass fraction / %	0	21.62	0	2.57	5.05	7.41
Viscosity under 25°C / (mm <sup>2</sup> ·s <sup>-1</sup> )	2.14	3.64	4.27	2.32	2.49	2.65
Theoretical air-fuel ratio	14.96	11.2	14.3	14.5	14.1	13.7

152

**Table 4.** Engine operating conditions

Category	Properties
Engine speed	1400 r/min
IMEP	About 0.85 MPa
Injection pressure	100 MPa
SOI	5 - 13 °CA BTDC

EGR ratio	0 - 30%
Inlet air temperature	25 ± 1°C
Cooling water temperature	80 ± 1°C

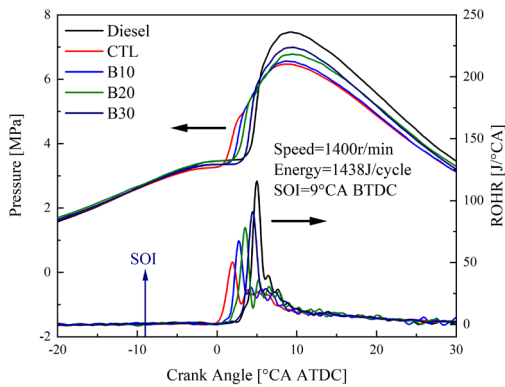
---

153 **3. Results and discussions**

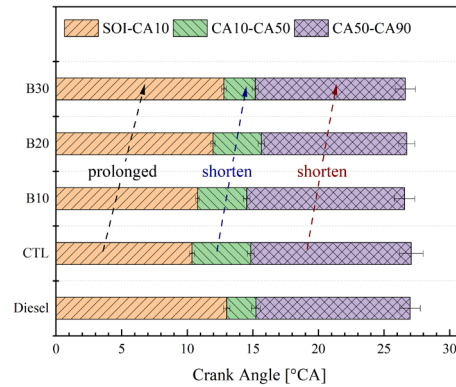
154 *3.1 Effects of CTL/n-butanol blends on combustion and emissions characteristics of the CI engine*

155 Compared with conventional diesel, CTL has higher CN, lower sulfur and aromatic content, so  
 156 it can be used to improve the combustion and emission performance of the CI engine. However,  
 157 applying pure CTL still has the problems of the slow combustion speed caused by the short ID.  
 158 Aiming at the problems of CTL combustion, n-butanol is blended into CTL to explore the way to  
 159 achieve the high-efficient and clean combustion of the CI engine.

160 *3.1.1 The effects of burning CTL/n-butanol blends on the combustion process*



(a) Cylinder pressure and HRR



(b) Combustion phasing

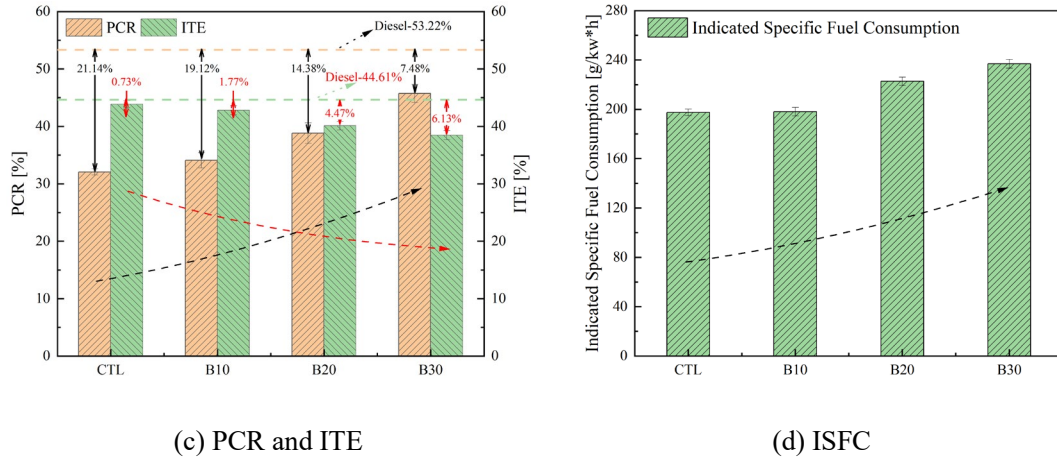


**Fig. 2** Comparison of the cylinder pressure, the HRR, the combustion characteristics, and ISFC in the cases of burning diesel, CTL, and CTL/n-butanol blends

161 In order to investigate the effects of blending n-butanol with CTL on the combustion process  
 162 of the CI engine, a comparative analysis of the combustion characteristics of diesel, CTL, and  
 163 CTL/n-butanol blends is carried out. **Fig. 2** shows the comparison of the cylinder pressure, the HRR,  
 164 and the combustion characteristics of diesel, CTL, and CTL/n-butanol blends. In this study part, the  
 165 SOI is fixed at 9°CA BTDC and, the EGR ratio is set to 0%. In **Fig. 2(b)**, the SOI-CA10 represents  
 166 the ID, and CA10-CA90 represents the combustion duration (CD). The CAXX represents the crank  
 167 angle (CA) at which the accumulated heat release reaches XX% of the entire cycle heat release, and  
 168 the HRR referred to in this article is the apparent heat release rate. This paper defines the premixed  
 169 combustion ratio (PCR) as the ratio of the cumulative heat release of the premixed combustion  
 170 endpoint (the crank angle corresponding to the minimum value of the heat release acceleration) to  
 171 the total cumulative heat release. It can be seen from **Fig. 2** that due to the higher CN and reactivity  
 172 meaning better ignitability, the CTL combustion has a shorter ID and a smaller PCR than those of  
 173 diesel, leading to the reduced peak value of HRR and cylinder pressure as well as the advanced  
 174 combustion phasing using CA50 as indicator. The HRR curves also show that applying CTL makes

175 the boundary between premixed and diffusion combustion more apparent, and the duration of  
176 diffusion combustion is significantly prolonged. Since premixed combustion speed is faster than  
177 that of diffusion combustion, the smaller PCR of CTL leads to a longer CD. The extended CD will  
178 reduce the propensity for constant volume combustion, leading to a decrease in the ITE. On the  
179 other hand, the inadequate premixed combustion is not conducive to the inhibition of particle  
180 generation.

181 In the interest of solving the problems of inadequate premixed combustion of burning pure  
182 CTL, n-butanol is blended with the CTL to reduce the reactivity of the in-cylinder fuel/air mixture  
183 and improve the homogeneity of the mixture. As illustrated in **Fig. 2**, the fuel reactivity decreases  
184 after adding n-butanol, resulting in a prolonged ID. Moreover, the addition of n-butanol with greater  
185 volatility is more conducive to forming the homogeneous mixture, so the PCR is significantly  
186 improved after the use of CTL/n-butanol blends. Compared with the pure CTL, the PCR of B10,  
187 B20, and B30 fuels increase by 2%, 6.76%, and 13.66%, respectively. At the same time, it can be  
188 observed from **Fig. 2(a)** that the high PCR causes an increase in the peak value of HRR and cylinder  
189 pressure. With the increase in the proportion of n-butanol from **Fig. 2(b)**, the reduced ignition  
190 performance and a larger latent heat of vaporization during the early atomization and vaporization  
191 process of the n-butanol have more noticeable effects on extending the ID, and the CA50 is  
192 postponed making the overall combustion phase more behind. From the perspective of the chemical  
193 reaction mechanism, alkanes produce a large number of OH radicals in the low-temperature reaction  
194 stage, and part of the OH radicals will be occupied and consumed by n-butanol. At this time, alkanes  
195 and n-butanol are in a competitive relationship to grab OH radicals, but the critical reaction is the  
196 dehydrogenation reaction between n-butanol and OH radicals suppressing ignition. Thereby, the

197 low-temperature ignition of the fuel is suppressed [42]. This phenomenon is more obvious with the  
198 increase in the proportion of n-butanol. Moreover, due to the addition of n-butanol, the PCR  
199 increased significantly, which considerably shortens the post-burning (CA50-CA90) duration  
200 reducing CD.

201 In general, increasing PCR contributes to the enhanced propensity for constant volume  
202 combustion to increase the ITE. However, it can be noticed from **Fig. 2(c)** that although blending  
203 n-butanol with CTL can effectively increase the PCR, the ITE of the engine decreases instead. The  
204 reason is that n-butanol has a higher latent heat of vaporization, which leads to a reduction of the  
205 cyclic heat release, and the addition of n-butanol also causes the combustion phasing to be delayed.  
206 The two reasons above harm the ITE corresponding to the fuel consumption rate from **Fig. 2(d)**.  
207 What can be seen is that the indicated specific fuel consumption (ISFC) of CTL, B10, B20 and B30  
208 are 197.4141g/kw\*h, 198.1227g/kw\*h, 222.7769g/kw\*h and 236.9085g/kw\*h, so fuel consumption  
209 rate has increased as the proportion of n-butanol increases.

### 210 *3.1.2 The effects of burning CTL/n-butanol blends on the emissions*

211 Blending n-butanol with CTL is beneficial to improving the homogeneity of fuel/air mixture  
212 and increasing the PCR, and the oxygen-containing molecular structure of n-butanol is helpful to  
213 reducing pollutant emissions. Accordingly, the emissions characteristics of diesel, CTL, and CTL/n-  
214 butanol blends are analyzed in this section.

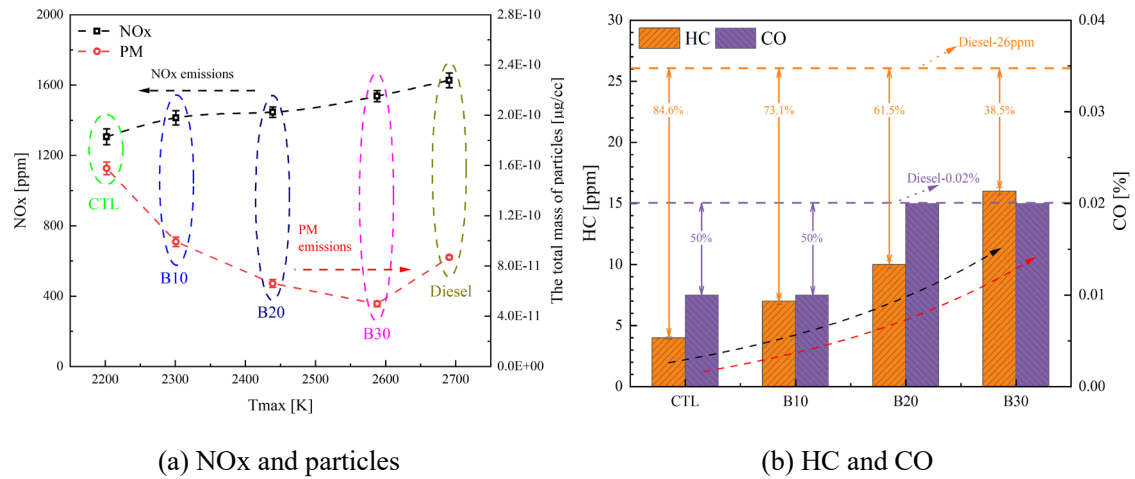


**Fig. 3** Influence of diesel, CTL, and CTL/n-butanol blends on engine emissions

215 Due to the trade-off relationship between NOx and particulate emissions, the emission control

216 of CI engines has always been a difficulty focused by researchers. The influence of diesel, CTL, and

217 CTL/n-butanol blends on NOx and particles is shown in Fig. 3(a). Since the maximum combustion

218 temperature is significantly affected by the premixed combustion, the order of the maximum

219 combustion temperature of different fuels is that CTL < B10 < B20 < B30 < diesel. The in-cylinder

220 high-temperature environment promotes NOx formation, so the NOx emissions of the engine

221 increase with the increase in the n-butanol blending ratio. However, all of the NOx emissions of

222 CTL/n-butanol are lower than that of diesel. The particles are more prone to be generated in the

223 environment of high-temperature and fuel-rich, which is more likely to appear during the process of

224 diffusion combustion [43]. Fig. 3(a) shows that blending n-butanol with the CTL effectively

225 suppresses the particulate emissions. The higher peak combustion temperature will promote the

226 initial generation of particulate matter in the local oxygen-lean area, but there is an obvious effect

227 on reducing particulate emissions by CTL/n-butanol blends. The addition of n-butanol into CTL can

228 prolong the ID and improve the concentration distribution of the fuel-gas mixture before ignition.

229 Besides, the n-butanol molecule has the property of oxygen containing, which is propitious to reduce

230 the local fuel-rich region in the combustion process. At the microscopic level, n-butanol contains  
231 OH radicals, which can be formed directly from n-butanol molecules by the cracking of the C-O  
232 bonds, while the alkane fuels need first to break C-H bonds to form active H ions and then combine  
233 with the O atoms in the air to form OH radicals. The OH radicals can effectively inhibit the  
234 generation of the soot precursor. Therefore, as the n-butanol blending ratio increases, the particulate  
235 emissions are reduced. Taken together, blending n-butanol with CTL mitigates the trade-off  
236 relationship between NO<sub>x</sub> and particulate emissions relative to diesel combustion. Accordingly, the  
237 NO<sub>x</sub> and particulate emissions obtained by using B30 fuel are reduced by 11.12% and 23.9%,  
238 respectively, compared to those of diesel fuel.

239 **Fig. 3(b)** presents the influence of diesel, CTL, and CTL/n-butanol blends on HC and CO  
240 emissions. As shown in **Fig. 3(b)**, the HC emissions gradually increase as the n-butanol blending  
241 ratio increases, but the B30 fuel still has lower HC emissions than diesel. This phenomenon is related  
242 to the change in the ID. The longer ID makes fuel adhere more easily to the cylinder wall, and the  
243 fuel distributing on the cylinder wall cannot be fully oxidized in the combustion process, resulting  
244 in higher HC emissions. Another reason for the lower HC emissions of CTL and CTL/n-butanol  
245 blends is that the low distillation temperature and high volatility of CTL lead to a reduction in the  
246 fuel-rich region of the cylinder, which also helps to suppress unburned HC emissions. **Fig. 3(b)** also  
247 illustrates that CO emissions rise with the increase of the n-butanol blending ratio but remain within  
248 the lower level.



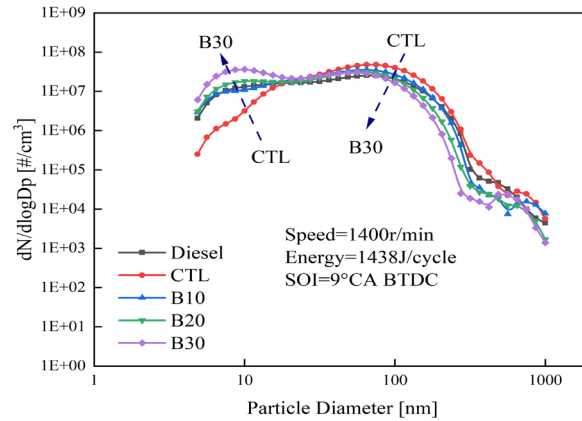


**Fig. 4** Influence of diesel, CTL, and CTL/n-butanol blends on particle size distribution

249 Since the particles in CI engines are complex in composition and cover a wide range of sizes,  
 250 the particle size distributions of diesel, CTL, and CTL/n-butanol blends are extracted as shown in  
 251 **Fig. 4**. The particles with a diameter smaller than 35 nm are defined as the nucleation mode particle  
 252 (NMP), and the particles with a diameter larger than 35 nm are defined as the accumulation mode  
 253 particle (AMP). It can be seen from **Fig. 4** that, with 35 nm as the demarcation point, the change  
 254 rules of NMP and AMP present an opposite trend. The reason is that the formation mechanisms of  
 255 different mode particles are discrepant. The NMP is mainly formed by the unburned HC during the  
 256 exhaust dilution and cooling, and the AMP is mainly generated by the aggregation of carbonaceous  
 257 particles produced by the dehydrocyclization of fuel in the region of high-temperature and fuel-rich  
 258 [44]. The combustion of CTL undergoes a larger proportion of diffusion combustion, so there are  
 259 more high-temperature and hypoxic regions in the combustion process. At the same time, the HC  
 260 emissions are lower when burning CTL. Thus, compared with diesel, fueling CTL in the CI engine  
 261 can significantly reduce the number of NMP, while the peak number of AMP significantly rises. As  
 262 the blending of n-butanol with CTL can improve the concentration distribution of fuel/air mixture  
 263 and its molecule contains oxygenated radicals, it can be found from **Fig. 4** that n-butanol blended

264 can help to suppress the higher AMP emission caused by the CTL combustion and promote the  
 265 shifting of particles towards NMP.

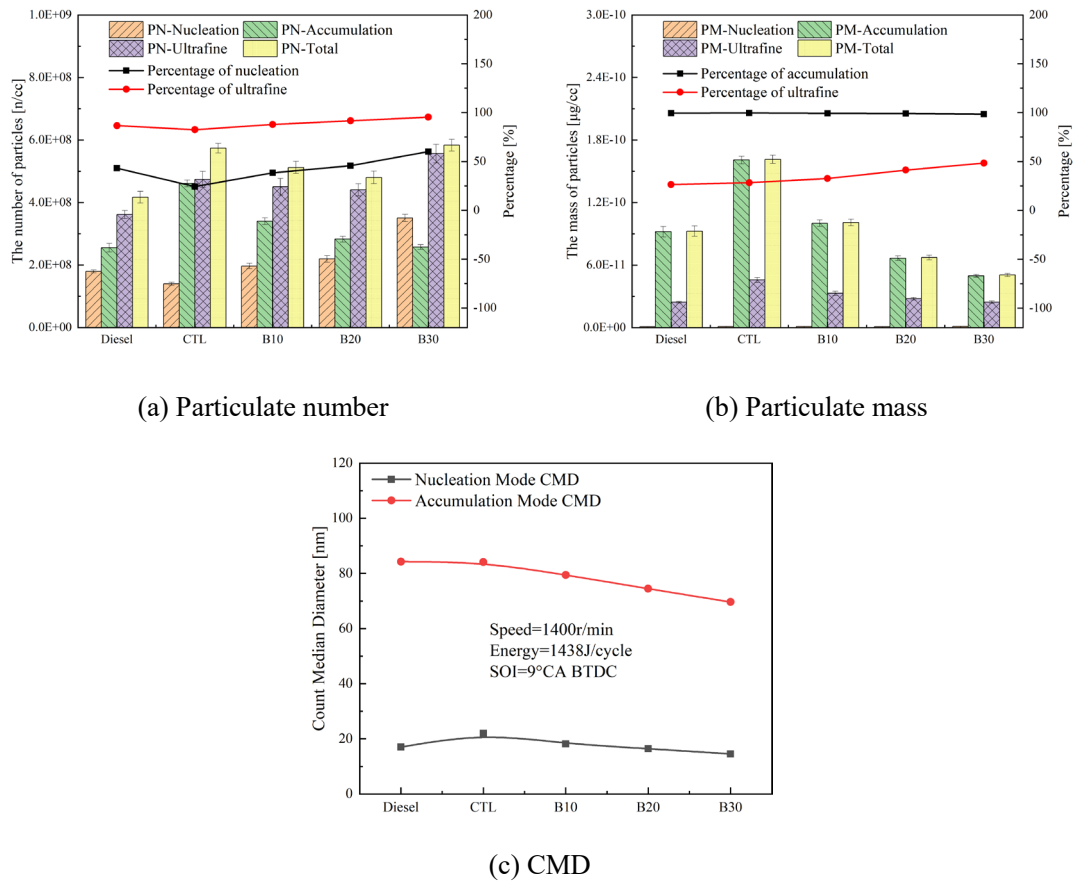


**Fig. 5** Influence of diesel, CTL, and CTL/n-butanol blends on different mode particles and

CMD

266 The earlier emission regulations only restricted the mass emission of particles, but in recent  
 267 years, the emission regulations have added limitations on the number emission of particles [45].  
 268 Therefore, number emissions, and mass emissions and CMD of different mode particles of diesel,  
 269 CTL, and CTL/n-butanol blends are further extracted, as shown in **Fig. 5**. The figure indicates that  
 270 the ultrafine particles (the particles with a diameter smaller than 100 nm) account for most of the  
 271 total particulate number (over 80% in all conditions), while the AMP mass is in the majority of the  
 272 total particulate mass (over 98% in all conditions). As depicted in **Fig. 5(a)**, compared with diesel,

273 when fueling CTL in the CI engine, the number of NMP decreases by 22.2%, the number of AMP  
274 increases by 80.7%, and the total particulate number and mass increases by 37.7% and 74.5%,  
275 respectively. The CTL/n-butanol blends effectively reduce the emission of AMP but lead to an  
276 increase in the number and proportion of NMP. Since the mass of AMP accounts for the majority of  
277 the total particulate mass, blending n-butanol with CTL can effectively reduce the particulate mass  
278 emissions. Compared to the total particulate mass emissions of the pure CTL, those of the B10, B20,  
279 and B30 fuel were reduced by 37.8%, 58.3%, and 68.6%, respectively. However, since the  
280 particulate number of the NMP and AMP shows an opposite trend with an increase in the n-butanol  
281 blending ratio, the total particle number emissions are not significantly affected by the addition of  
282 n-butanol. At the same time, the particulate size characteristics of the above test fuels can also be  
283 reflected in the changing trend of CMD in **Fig. 5(c)**. It can be seen from the figure that, although  
284 the above conclusions indicate that CTL particulate matter emissions are relatively high, ultrafine  
285 particles account for a relatively large proportion for CTL, making its accumulation mode CMD the  
286 same as diesel. Moreover, with the addition of n-butanol in the CTL, both nucleation mode CMD  
287 and accumulation mode CMD decrease significantly with n-butanol ratio increasing. In particular,  
288 the decline of accumulation mode CMD is evident compared with pure hydrocarbon fuels such as  
289 diesel and CTL, demonstrating that the addition of n-butanol has a noticeable effect on inhibiting  
290 the AMP produced by CTL. For example, the degree of reduction of accumulation mode CMD of  
291 B30 reaches 17.37% compared with pure CTL.

### 292 *3.2 Effects of fuel injection strategy on the combustion and emissions of the CTL/n-butanol blends* 293 *engine*

294 In order to obtain a suitable fuel injection strategy for the CTL/n-butanol blends engine, the

295 effects of fuel injection conditions on the combustion process and primary emissions of the engine

296 fueled the CTL/n-butanol blends are investigated in this section.

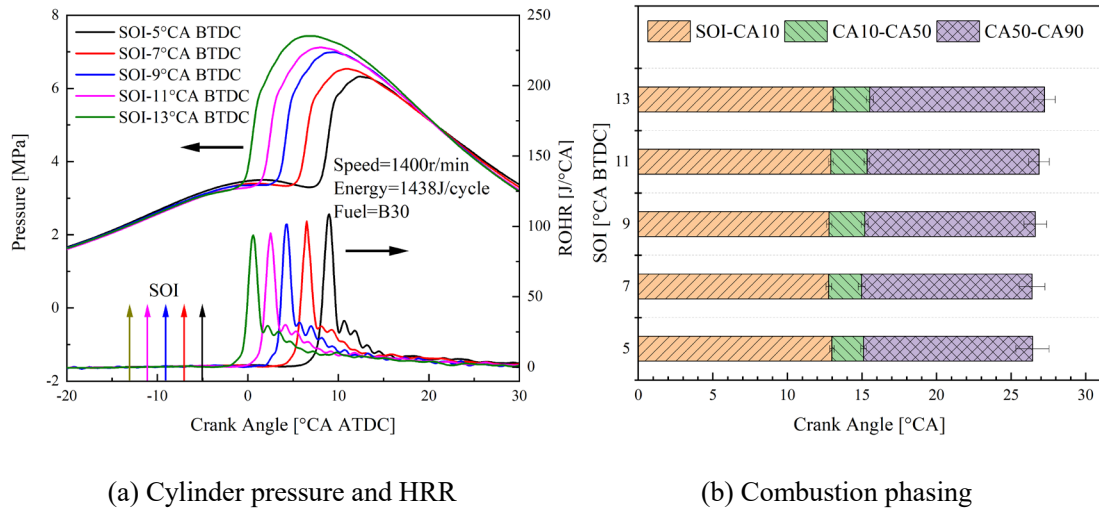


**Fig. 6** Influence of SOI on the combustion process when burning B30 fuel

297 **Fig. 6** shows the influence of SOI on the combustion process when burning B30 fuel. What  
298 can be observed from **Fig. 6** is that, as the SOI advances, the ID remains almost constant, so the  
299 ignition timing is advanced, and the combustion process is closer to the top dead center (TDC).  
300 Since the cylinder volume decreases as the piston gets closer to the TDC, the maximum cylinder  
301 pressure increases with the advance of the SOI. However, as the SOI advances, the HRR curves  
302 move forward while the shapes remain approximately the same. Since the higher temperature and  
303 pressure near the TDC facilitate the combustion process, early injection slightly shortens the CD.

304 Since the addition of n-butanol and SOI both have a significant influence on the combustion  
305 process of the engine and thus on the ITE, the influence of the injection strategy on the ITE of the  
306 engine fueled CTL/n-butanol blends is shown in **Fig. 7**. The early injection will cause the  
307 combustion process to approach the TDC, which is conducive to improving the propensity for  
308 constant volume combustion. Hence, the figure presents that the advanced injection contributes to

309 enhancing the ITE. However, blending n-butanol with CTL causes a decrease in ITE due to the high  
 310 latent heat of vaporization and the postponed combustion. Among them, the effect of n-butanol  
 311 blended on ITE is more significant than adjusting the SOI. The ITE is increased by about 2% after  
 312 advancing the SOI from 5 °CA BTDC to 13 °CA BTDC for all fuels. At the same SOI, the ITE is  
 313 reduced by about 5% after increasing the n-butanol blending ratio from 0% to 30%. It indicates that  
 314 the SOI needs to be advanced by about 6 °CA to recover the ITE degradation caused by the 10% n-  
 315 butanol addition.

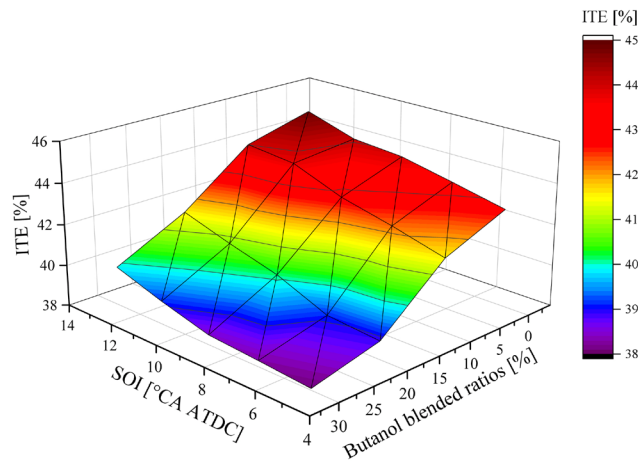
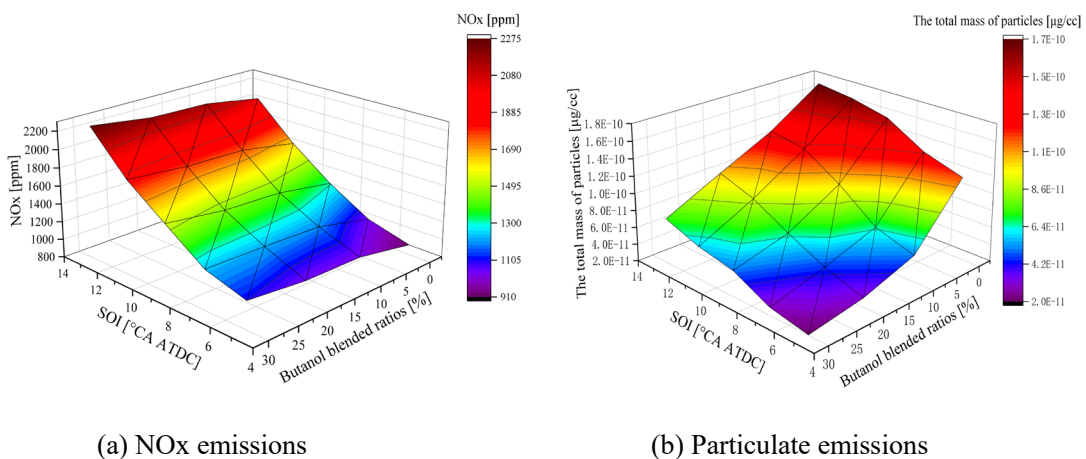


**Fig. 7** Influence of injection strategy on the ITE of the CTL/n-butanol blends engine



(a) NOx emissions

(b) Particulate emissions

**Fig. 8** Influence of injection strategy on the emissions of the CTL/n-butanol blends engine

316 **Fig. 8** demonstrates the influence of injection strategy on the NOx and particulate emissions

317 of the CTL/n-butanol blends. As can be observed from **Fig. 8(a)**, the advanced injection or  
318 increasing the n-butanol blending ratio can both lead to an increase in NO<sub>x</sub> emissions, and the  
319 influence of SOI on NO<sub>x</sub> emissions is far more significant than that of n-butanol addition. The NO<sub>x</sub>  
320 emissions are increased by about 1150 ppm after advancing the SOI from 5 °CA BTDC to 13 °CA  
321 BTDC for all fuels. At the same SOI, the NO<sub>x</sub> emissions are increased by about 210 ppm after  
322 increasing the n-butanol blending ratio from 0% to 30%. The reason is that the advanced injection  
323 and the n-butanol addition both make the combustion process close to the TDC, which leads to a  
324 rising combustion temperature and promote the generation of NO<sub>x</sub> emissions, but the influence of  
325 the change in SOI is much greater than that of blending n-butanol. As shown in Fig. 8(b), the addition  
326 of n-butanol significantly reduces particulate emissions, while the higher temperature brought by  
327 advanced SOI leads to an increase in particulate emissions, and the effect of blending n-butanol on  
328 particulate emissions is more obvious. Consequently, the particulate emission of CTL increases by  
329 49.5% after advancing the SOI from 5 °CA BTDC to 13 °CA BTDC. At the SOI of 5 °CA BTDC,  
330 the particulate emission is reduced by 82.7% after the n-butanol proportion is increased from 0% to  
331 30%.

### 332 *3.3 Effects of EGR on ITE and emissions of the CTL/n-butanol blends engine*

333 In order to control the increased NO<sub>x</sub> emissions caused by the addition of n-butanol, the  
334 introduction of EGR was adopted to control NO<sub>x</sub> emissions. The potential for high-efficient and  
335 clean combustion through the synergistic control of EGR and the addition of n-butanol is explored.

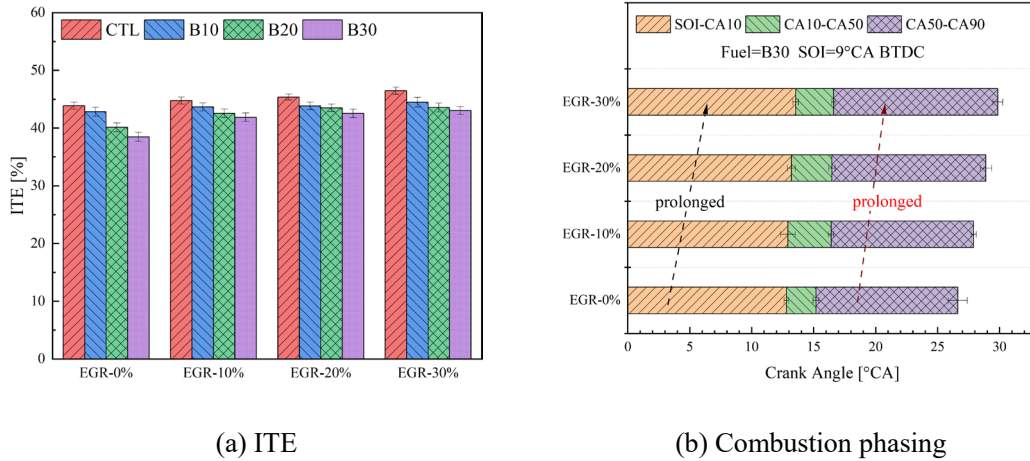
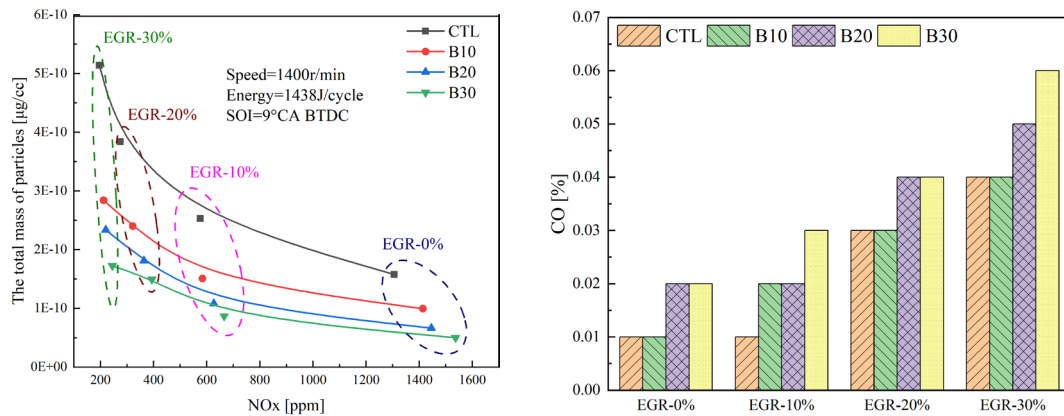


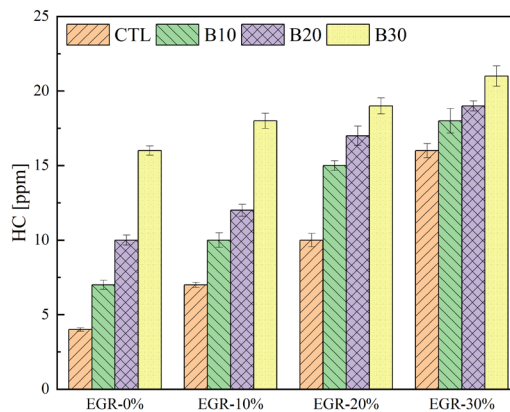
**Fig. 9** Influence of EGR on the ITE and combustion phasing of the CTL/n-butanol blends engine

336 **Fig. 9** presents the influence of EGR on ITE and combustion phasing, respectively. As shown  
 337 in **Fig. 9(a)**, the ITE is reduced with the increase of n-butanol proportion at all EGR ratios. Since  
 338 the EGR ratio is adjusted by introducing the exhaust flow while keeping the flow of intake air  
 339 constant through the simulated supercharge system in this experiment, the high EGR ratio increases  
 340 intake pressure and charge. The high intake pressure and the heat introduced by the EGR bring extra  
 341 work, so an increasing EGR ratio will result in a slightly higher ITE. However, the three-atomic  
 342 molecules ( $H_2O$ ,  $CO_2$ ) contained in the EGR have a higher specific heat capacity (SHC) than the  
 343 two-atomic molecules ( $O_2$ ,  $N_2$ ) in the air, so the introduction of EGR can effectively reduce the in-  
 344 cylinder combustion temperature. **Fig. 9(b)** shows the combustion phasing of B30 under different  
 345 EGR ratios. It can be found that with the EGR ratio increasing, the ID increases slightly, but the lag  
 346 of CA50 is even more significant. The introduction of EGR reduces the oxygen concentration in the  
 347 cylinder, further reducing the reaction activity and temperature of the mixture, so the combustion at  
 348 middle and later stages (CA10-CA90) is slowed down, resulting in a more extended CD.



(a) NOx and particulate emissions

(b) CO



(c) HC

349

**Fig. 10** Influence of EGR on the emissions of the CTL/n-butanol blends engine

350

**Fig. 10** suggests that the influence of EGR on emissions of the CTL/n-butanol blends engine.

351

**Fig. 10(a)** illustrates that the introduction of EGR significantly reduces the high NOx emissions

352

associated with the addition of n-butanol. Simultaneously, due to the enhanced tolerance of

353

particulate emissions to EGR by blending CTL with n-butanol, the introduction of EGR would not

354

lead to an excessive increase in particulate emissions. Therefore, the trade-off relationship between

355

NOx and particulate emissions can be mitigated through the synergistic control of EGR and the

356

addition of n-butanol. Among them, the NOx and particulate emissions of using B30 at 10% EGR

357

are reduced by 45.1% and 49%, respectively, compared to those of using pure CTL with no EGR

358

introduced. **Figs. 10(b)** and **(c)** show the CO and HC emissions of the test fuels at different EGR



359 ratios, respectively. At a fixed EGR ratio, the changing trend of CO and HC emission results for  
360 different test fuels is the same as in section 3.1.2. It can be seen from **Fig. 10(b)** that CO emissions  
361 increase as more EGR introducing, and this phenomenon is more obvious for CTL/n-butanol blends.  
362 The main reasons are that the addition of n-butanol causes the combustion duration to be longer,  
363 and the combustion phasing is too backward. Especially when the n-butanol proportion becomes  
364 larger, the combustion efficiency is reduced, leading the CO emissions to be relatively high. It also  
365 can be seen from **Fig. 10(c)** that although the HC emissions become higher with the n-butanol  
366 proportion rising, the HC increasing degree of the blends is much smaller than that of the pure CTL  
367 with an enlarged EGR ratio. For example, when the EGR ratio changes from 0% to 30%, the HC  
368 increasing degree of B30 is 31.25% while the CTL reaches 300%, indicating that the addition of n-  
369 butanol can improve the tolerance of HC emissions to the EGR ratio.

#### 370 **4. Conclusions**

371 In this paper, the effects of the CTL/n-butanol blends on the combustion and emissions of the  
372 CI engine are investigated on a modified engine with flexible and adjustable control parameters,  
373 and the potential for reducing pollutant emissions from CTL/n-butanol blends by adjusting  
374 combustion boundary conditions is explored. The main findings can be summarized as follows:

375 (1) Compared to conventional diesel, CTL has higher reactivity which means better ignitability  
376 helping to shorten the ID. The PCR of CTL is smaller than that of diesel, and the boundary between  
377 the premixed and the diffusion combustion is more apparent. Accordingly, applying CTL can reduce  
378 NO<sub>x</sub> emissions but has higher particulate mass emissions.

379 (2) The improved concentration distribution of fuel/air mixture brought by the addition of n-  
380 butanol and the oxygen-containing property of n-butanol contributes to suppressing the high

381 particulate emissions caused by pure CTL combustion and promoting the shifting of particles  
382 towards nucleation mode, thus effectively reducing the total particulate mass emissions. At the same  
383 time, blending n-butanol with the CTL increases the PCR and the maximum combustion  
384 temperature, which results in higher NO<sub>x</sub> emissions, although it is still lower than the condition of  
385 pure diesel combustion.

386 (3) Adjusting the SOI mainly affects the combustion phase but slightly changes the ID and the  
387 shapes of HRR curves. Compared with the addition of n-butanol, adjusting the SOI has a marked  
388 effect on NO<sub>x</sub> emissions while has a minor influence on the ITE and particulate emissions.

389 (4) The introduction of EGR can significantly reduce the increased NO<sub>x</sub> emissions caused by  
390 the addition of n-butanol, and the tolerance of particulate emissions and HC to EGR is improved  
391 after blending n-butanol with CTL. Through the coordinated control of EGR and the addition of n-  
392 butanol, the trade-off relationship between NO<sub>x</sub> and particulate emissions can be mitigated.

393

#### 394 **Notes**

395 The authors declare no competing financial interest.

#### 396 **Acknowledgments**

397 This work was supported by the National Natural Science Foundation of China (Project code:  
398 51476069, 51676084); Jilin Provincial Industrial Innovation Special Guidance Fund Project (Project  
399 code: 2019C058-3); Jilin Province Science and Technology Development Plan Project (Project code:  
400 20180101059JC); Jilin Province Specific Project of Industrial Technology Research &  
401 Development (Project code: 2020C025-2); Jilin University Ph.D. Interdisciplinary Research

402 Funding Project (Project code:101832020DJX040).

403

## 404 **References**

405 [1] Dernote J, Mounaim-Rousselle C, Halter F, Seers P. Evaluation of Butanol–Gasoline Blends in  
406 a Port Fuel-injection, Spark-Ignition Engine. Oil Gas Sci Technol – Rev IFP. 2010;65(2):345-51.

407 <https://doi.org/10.2516/ogst/2009034>

408 [2] Awad OI, Mamat R, Ali OM, Sidik NAC, Yusaf T, Kadirgama K, et al. Alcohol and ether as  
409 alternative fuels in spark ignition engine: A review. Renewable and Sustainable Energy Reviews.

410 2018;82:2586-605. <https://doi.org/10.1016/j.rser.2017.09.074>

411 [3] Karavalakis G, Short D, Hajbabaie M, Vu D, Villela M, Russell R, et al. Criteria Emissions,  
412 Particle Number Emissions, Size Distributions, and Black Carbon Measurements from PFI Gasoline  
413 Vehicles Fuelled with Different Ethanol and Butanol Blends. SAE International; 2013.

414 <https://doi.org/10.4271/2013-01-1147>

415 [4] Vancoillie J, Sileghem L, Van de Ginste M, Demuyneck J, Galle J, Verhelst S. Experimental  
416 Evaluation of Lean-burn and EGR as Load Control Strategies for Methanol Engines. SAE

417 International; 2012. <https://doi.org/10.4271/2012-01-1283>

418 [5] Othman MF, Adam A, Najafi G, Mamat R. Green fuel as alternative fuel for diesel e  
419 ngine: A review. Renewable and Sustainable Energy Reviews. 2017;80:694-709. [https://doi.o](https://doi.org/10.1016/j.rser.2017.05.140)

420 [rg/10.1016/j.rser.2017.05.140](https://doi.org/10.1016/j.rser.2017.05.140)

421 [6] Baruch JJ. Combating global warming while enhancing the future. Technology in Society.

422 2008;30(2):111-21. <https://doi.org/10.1016/j.techsoc.2007.12.008>

- 423 [7] Allen, Barros V, Broome J, Cramer W, Christ R, Church J, et al. Climate Change 2014: Synthesis  
424 Report2014. <https://doi.org/10.1111/j.1728-4457.2001.00203.x>
- 425 [8] Liu Z, Zhang H, Hao H, Zhao F. Comparative study of corporate average fuel consumption  
426 regulations based on curb weight and footprint benchmarks. Clean Technologies and Environmental  
427 Policy. 2020;22(6):1311-23. <https://doi.org/10.1007/s10098-020-01872-5>
- 428 [9] Winkler S, Anderson J, Garza L, Ruona W, Vogt R, Wallington T. Vehicle criteria pollutant (PM,  
429 NO<sub>x</sub>, CO, HCs) emissions: how low should we go? npj Climate and Atmospheric Science. 2018;1.  
430 <https://doi.org/10.1038/s41612-018-0037-5>
- 431 [10] Ryan Walker N, Wissink ML, DeVescovo DA, Reitz RD. Natural Gas for High Load Dual-  
432 Fuel Reactivity Controlled Compression Ignition in Heavy-Duty Engines. Journal of Energy  
433 Resources Technology. 2015;137(4). <https://doi.org/10.1115/1.4030110>
- 434 [11] Castro N, Toledo M, Amador G. An experimental investigation of the performance and  
435 emissions of a hydrogen-diesel dual fuel compression ignition internal combustion engine. Applied  
436 Thermal Engineering. 2019;156:660-7. <https://doi.org/10.1016/j.applthermaleng.2019.04.078>
- 437 [12] Ong HC, Masjuki HH, Mahlia TMI, Silitonga AS, Chong WT, Yusaf T. Engine performance  
438 and emissions using Jatropha curcas, Ceiba pentandra and Calophyllum inophyllum biodiesel in a  
439 CI diesel engine. Energy. 2014;69:427-45. <https://doi.org/10.1016/j.energy.2014.03.035>
- 440 [13] Du J, Sun W, Wang X, Li G, Tan M, Fan L. Experimental study on combustion and particle  
441 size distribution of a common rail diesel engine fueled with GTL/diesel blends. Applied Thermal  
442 Engineering. 2014;70(1):430-40. <https://doi.org/10.1016/j.applthermaleng.2014.05.037>
- 443 [14] Pei Y, Qin J, Dai Y, Wang K. Investigation on the spray development, the combustion  
444 characteristics and the emissions of Fischer–Tropsch fuel and diesel fuel from direct coal

445 liquefaction. Proceedings of the Institution of Mechanical Engineers, Part D: Journal of Automobile  
446 Engineering. 2017;231(13):1829-37. <https://doi.org/10.1177/0954407016687861>

447 [15] van Vliet OPR, Faaij APC, Turkenburg WC. Fischer–Tropsch diesel production in a well-to-  
448 wheel perspective: A carbon, energy flow and cost analysis. Energy Conversion and Management.  
449 2009;50(4):855-76. <https://doi.org/10.1016/j.enconman.2009.01.008>

450 [16] Hao X, Dong G, Yang Y, Xu Y, Li Y. Coal to Liquid (CTL): Commercialization Pro  
451 spects in China. Chemical Engineering & Technology. 2007;30(9):1157-65. [https://doi.org/10.](https://doi.org/10.1002/ceat.200700148)  
452 [1002/ceat.200700148](https://doi.org/10.1002/ceat.200700148)

453 [17] Mantripragada HC, Rubin ES. CO2 reduction potential of coal-to-liquids (CTL) proces  
454 s: Effect of gasification technology. Energy Procedia. 2011;4:2700-7. [https://doi.org/10.1016/](https://doi.org/10.1016/j.egypro.2011.02.171)  
455 [j.egypro.2011.02.171](https://doi.org/10.1016/j.egypro.2011.02.171)

456 [18] Man Y, Xiao H, Cai W, Yang S. Multi-scale sustainability assessments for biomass-based and  
457 coal-based fuels in China. Science of The Total Environment. 2017;599-600:863-72.  
458 <https://doi.org/10.1016/j.scitotenv.2017.05.006>

459 [19] Jin C, Mao B, Dong F, Liu X, Yang Y, Chen P, et al. Effects of Indirect and Direct  
460 Coal-to-Liquid Fuel on Combustion, Performance, and Emissions in a Six-Cylinder Heavy  
461 -Duty Diesel Engine. Journal of Energy Engineering. 2018;144(3):04018024. [https://doi.org/](https://doi.org/10.1061/(ASCE)EY.1943-7897.0000531)  
462 [10.1061/\(ASCE\)EY.1943-7897.0000531](https://doi.org/10.1061/(ASCE)EY.1943-7897.0000531)

463 [20] Campos A, Lohitharn N, Roy A, Lotero E, Goodwin JG, Spivey JJ. An activity and XANES  
464 study of Mn-promoted, Fe-based Fischer–Tropsch catalysts. Applied Catalysis A: General.  
465 2010;375(1):12-6. <https://doi.org/10.1016/j.apcata.2009.11.015>

466 [21] Shi JH, Wang T, Zhao Z, Yang TT, Zhang ZW. Experimental Study of Injection Parameters on

467 the Performance of a Diesel Engine with Fischer-Tropsch Fuel Synthesized from Coal. *Energies*.  
468 2018;11(12):11. <https://doi.org/10.3390/en11123280>

469 [22] Hao B, Song C, Lv G, Li B, Liu X, Wang K, et al. Evaluation of the reduction in carbonyl  
470 emissions from a diesel engine using Fischer–Tropsch fuel synthesized from coal. *Fuel*.  
471 2014;133:115-22. <https://doi.org/10.1016/j.fuel.2014.05.025>

472 [23] Gill SS, Tsolakis A, Dearn KD, Rodríguez-Fernández J. Combustion characteristics and  
473 emissions of Fischer–Tropsch diesel fuels in IC engines. *Progress in Energy and Combustion*  
474 *Science*. 2011;37(4):503-23. <https://doi.org/10.1016/j.pecs.2010.09.001>

475 [24] Song C, Gong G, Song J, Lv G, Cao X, Liu L, et al. Potential for Reduction of Ex  
476 haust Emissions in a Common-Rail Direct-Injection Diesel Engine by Fueling with Fischer  
477 –Tropsch Diesel Fuel Synthesized from Coal. *Energy & Fuels*. 2012;26(1):530-5. <https://doi.org/10.1021/ef201378r>

478

479 [25] Dai YL, Pei YQ, Qin J, Zhang JY, Li YL. Experimental Study of Coal Liquefaction  
480 Diesel Combustion and Emissions. *Applied Mechanics and Materials*. 2013;291-294:1914-9.  
481 <https://doi.org/10.4028/www.scientific.net/AMM.291-294.1914>

482 [26] Devarajan Y, Beemkumar N, Ganesan S, Arunkumar T. An experimental study on the influence  
483 of an oxygenated additive in diesel engine fuelled with neat papaya seed biodiesel/diesel blends.  
484 *Fuel*. 2020;268:117254. <https://doi.org/10.1016/j.fuel.2020.117254>

485 [27] Deh Kiani MK, Ghobadian B, Tavakoli T, Nikbakht AM, Najafi G. Application of artificial  
486 neural networks for the prediction of performance and exhaust emissions in SI engine using ethanol-  
487 gasoline blends. *Energy*. 2010;35(1):65-9. <https://doi.org/10.1016/j.energy.2009.08.034>

488 [28] Rakopoulos DC, Rakopoulos CD, Kyritsis DC. Butanol or DEE blends with either straight

489 vegetable oil or biodiesel excluding fossil fuel: Comparative effects on diesel engine combustion  
490 attributes, cyclic variability and regulated emissions trade-off. *Energy*. 2016;115:314-25.  
491 <https://doi.org/10.1016/j.energy.2016.09.022>

492 [29] Zuo Q, Zhu X, Liu Z, Zhang J, Wu G, Li Y. Prediction of the performance and emi  
493 ssions of a spark ignition engine fueled with butanol-gasoline blends based on support vec  
494 tor regression. *Environmental Progress & Sustainable Energy*. 2019;38(3):e13042. [https://doi.](https://doi.org/10.1002/ep.13042)  
495 [org/10.1002/ep.13042](https://doi.org/10.1002/ep.13042)

496 [30] Gu X, Huang Z, Cai J, Gong J, Wu X, Lee C-f. Emission characteristics of a spark-ignition  
497 engine fuelled with gasoline-n-butanol blends in combination with EGR. *Fuel*. 2012;93:611-7.  
498 <https://doi.org/10.1016/j.fuel.2011.11.040>

499 [31] Nour M, Attia AMA, Nada SA. Combustion, performance and emission analysis of diesel  
500 engine fuelled by higher alcohols (butanol, octanol and heptanol)/diesel blends. *Energy Conversion*  
501 *and Management*. 2019;185:313-29. <https://doi.org/10.1016/j.enconman.2019.01.105>

502 [32] Atmanli A. Comparative analyses of diesel–waste oil biodiesel and propanol, n-butano  
503 l or 1-pentanol blends in a diesel engine. *Fuel*. 2016;176:209-15. [https://doi.org/10.1016/j.fu](https://doi.org/10.1016/j.fuel.2016.02.076)  
504 [el.2016.02.076](https://doi.org/10.1016/j.fuel.2016.02.076)

505 [33] Jin C, Yao M, Liu H, Lee C-f, Ji J. Progress in the production and application of  
506 n-butanol as a biofuel. *Renewable and Sustainable Energy Reviews*. 2011;15(8):4080-106. [h](https://doi.org/10.1016/j.rser.2011.06.001)  
507 [tps://doi.org/10.1016/j.rser.2011.06.001](https://doi.org/10.1016/j.rser.2011.06.001)

508 [34] Soloiu V, Duggan M, Harp S, Vlcek B, Williams D. PFI (port fuel injection) of n-butanol and  
509 direct injection of biodiesel to attain LTC (low-temperature combustion) for low-emissions idling  
510 in a compression engine. *Energy*. 2013;52:143-54. <https://doi.org/10.1016/j.energy.2013.01.023>

- 511 [35] Huang H, Zhou C, Liu Q, Wang Q, Wang X. An experimental study on the combustion and  
512 emission characteristics of a diesel engine under low temperature combustion of diesel/gasoline/n-  
513 butanol blends. *Applied Energy*. 2016;170:219-31. <https://doi.org/10.1016/j.apenergy.2016.02.126>
- 514 [36] Chen Z, Liu J, Han Z, Du B, Liu Y, Lee C. Study on performance and emissions o  
515 f a passenger-car diesel engine fueled with butanol–diesel blends. *Energy*. 2013;55:638-46.  
516 <https://doi.org/10.1016/j.energy.2013.03.054>
- 517 [37] Siwale L, Kristóf L, Adam T, Bereczky A, Mbarawa M, Penninger A, et al. Combustion and  
518 emission characteristics of n-butanol/diesel fuel blend in a turbo-charged compression ignition  
519 engine. *Fuel*. 2013;107:409-18. <https://doi.org/10.1016/j.fuel.2012.11.083>
- 520 [38] Tüccar G, Özgür T, Aydın K. Effect of diesel–microalgae biodiesel–butanol blends on  
521 performance and emissions of diesel engine. *Fuel*. 2014;132:47-52. <https://doi.org/10.1016/j.fuel.2014.04.074>
- 522 [fuel.2014.04.074](https://doi.org/10.1016/j.fuel.2014.04.074)
- 523 [39] Rajesh Kumar B, Saravanan S. Effects of iso-butanol/diesel and n-pentanol/diesel blends on  
524 performance and emissions of a DI diesel engine under premixed LTC (low temperature combustion)  
525 mode. *Fuel*. 2016;170:49-59. <https://doi.org/10.1016/j.fuel.2015.12.029>
- 526 [40] Chen Z, Wu Z, Liu J, Lee C. Combustion and emissions characteristics of high n-butanol/diesel  
527 ratio blend in a heavy-duty diesel engine and EGR impact. *Energy Conversion and Management*.  
528 2014;78:787-95. <https://doi.org/10.1016/j.enconman.2013.11.037>
- 529 [41] Huang H, Liu Q, Wang Q, et al. Experimental investigation of particle emissions under different  
530 EGR ratios on a diesel engine fueled by blends of diesel/gasoline/n-butanol. *Energy Conversion and*  
531 *Management*. 2016; 121; 212-223. <https://doi.org/10.1016/j.enconman.2016.05.034>
- 532 [42] Zhu J, Huang H, Zhu Z, et al. Effect of intake oxygen concentration on diesel–n-butanol



533 blending combustion: An experimental and numerical study at low engine load. *Energy Conversion*  
534 and Management, 2018, 165(6): 53-65. <https://doi.org/10.1016/j.enconman.2018.03.045>

535 [43] Li Z, Song C, Song J, Lv G, Dong S, Zhao Z. Evolution of the nanostructure, fractal dimension  
536 and size of in-cylinder soot during diesel combustion process. *Combustion and Flame*.  
537 2011;158(8):1624-30. <https://doi.org/10.1016/j.combustflame.2010.12.006>

538 [44] Wang Q, Sun W, Guo L, Fan L, Cheng P, Li G, et al. Particle number size distribution from  
539 direct-injection premixed combustion engine fueled with gasoline/diesel blends. *Proceedings of the*  
540 *Institution of Mechanical Engineers, Part D: Journal of Automobile Engineering*. 2019;234(1):258-  
541 69. <https://doi.org/10.1177/0954407019838128>

542 [45] Fujitani Y, Takahashi K, Fushimi A, Hasegawa S, Kondo Y, Tanabe K, et al. Particle  
543 number emission factors from diesel trucks at a traffic intersection: Long-term trend and  
544 relation to particle mass-based emission regulation. *Atmospheric Environment: X*. 2020;5:10  
545 0055. <https://doi.org/10.1016/j.aeaoa.2019.100055>